Bioorganic & Medicinal Chemistry 21 (2013) 7194–7201

Contents lists available at ScienceDirect

Bioorganic & Medicinal Chemistry

journal homepage: www.elsevier.com/locate/bmc

CoMFA studies and in vitro evaluation of some 3-substituted benzylthio quinolinium salts as anticryptococcal agents

Sidney Bolden [a], Comfort A. Boateng [a], Xue Y. Zhu [a], Jagan R. Etukala [a], Suresh K. Eyunni [a], Melissa R. Jacob [b], Shabana I. Khan [b], Seth Y. Ablordeppey [a,*]

[a] College of Pharmacy and Pharmaceutical Sciences, Florida A&M University, Tallahassee, FL 32307, USA
[b] The National Center for the Development of Natural Products, Research Institute of Pharmaceutical Sciences, University of Mississippi, University, MS 38677, USA

ARTICLE INFO

Article history:
Received 1 July 2013
Revised 14 August 2013
Accepted 23 August 2013
Available online 3 September 2013

Keywords:
CoMFA
Antifungal agents
Cryptolepine
Mycoses
Opportunistic infection
Substituted benzylthioquinolinium salts

ABSTRACT

The 3-dimensional quantitative structure–activity relationship (3D-QSAR) molecular modeling technique or comparative molecular field analysis (CoMFA) has been used to design analogs of the natural product cryptolepine (**1**). Twenty-three compounds with their in vitro biological activities (IC_{50} values) against *Crytococcus neoformans* were used to generate the training set database of compounds for the CoMFA studies. The cross-validated q^2, noncross-validated r^2, and partial least squares (PLS) analysis results were used to predict the biological activity of 11 newly designed test set compounds. The best CoMFA model produced a q^2 of 0.815 and an r^2 of 0.976 indicating high statistical significance as a predictive model. The steric and electrostatic contributions from the contour map were interpreted from the color-coded contour plots generated from the PLS model and the active structural components for potency against *C. neoformans* were determined and validated in the test set compounds. The 3-substituted benzylthio quinolinium salts (**4**) that make up the test set were synthesized and evaluated based on the predicted activity from the CoMFA model and the results produced a good correlation between the predicted and experimental activity ($R = 0.82$). Thus, CoMFA has served as an effective tool to aid the design of new analogs and in this case, it has aided the identification of compounds equipotent with amphotericin B, the gold standard in antifungal drug design.

Published by Elsevier Ltd.

1. Introduction

The incidence of opportunistic infections (OIs) has moderated lately due to the declining incidence of HIV AIDS in especially the developed countries.[1] However, OIs continue to be of public health concern. OIs occur when microorganisms that are well controlled in healthy individuals become unchecked in patients with compromised immune systems weakened by disease or medication. Consequently, as the number of people contracting HIV/AIDS, or undergoing chemotherapy, or receiving organ transplants increases, so does the risk of being infected by a pathogenic fungi.[2] The most common OIs include *Candida albicans*, *Aspergillus fumigatus* and *Cryptococcus neoformans* (*Cn*).[3] While there are several drugs against these OIs, many opportunistic fungi have developed resistance to drugs that have been on the market for an extended period of time such as fluconazole and nonliposomal amphotericin B.[4] In addition, the supply of new antifungal drugs with unique targets against OIs is behind the demand for new drugs that address the problem of resistance and side-effects among pathogenic fungi.[4]

The natural product cryptolepine (CLP, **1**, Fig. 1), obtained from the African climbing shrub *Cryptolepis sanguinolenta*, was previously shown to have interesting biological activities against a broad array of fungal and bacterial species, and operates through a unique mechanism of action.[5,6] During optimization of cryptolepine to improve its anti-infective properties, several resulting analogs have demonstrated increased potency and lower cytotoxicity than CLP.[7–11] These analogs span six different scaffolds and have generated important structure–activity relationship (SAR) data. The encouraging progress made during the optimization process spurred a need to develop a CoMFA model that would enable the prediction of subsequently designed analogs prior to their synthesis and thus, aid in the prioritization of the synthesis of designed analogs. The observation of a strong correlation, having used different chemotypes, would also provide the first indications that the compounds may be acting through a similar mechanism in inhibiting or killing the microorganisms. Thus, in this study, we report a CoMFA model that is able to predict the biological activity of new analogs based on their steric and electrostatic properties using a training set of 23 compounds. In addition, 11 new compounds designed to probe the electronic and hydrophobic space around the phenyl ring A, were synthesized and their inhibitory potencies

* Corresponding author. Tel.: +1 850 599 3834; fax: +1 850 599 3934.
E-mail address: seth.ablordeppey@famu.edu (S.Y. Ablordeppey).

0968-0896/$ - see front matter Published by Elsevier Ltd.
http://dx.doi.org/10.1016/j.bmc.2013.08.043

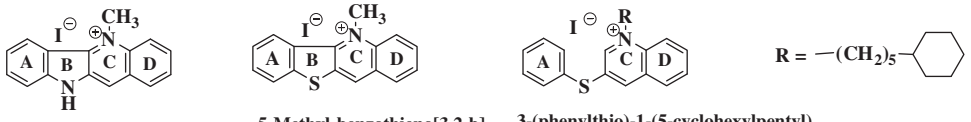

Figure 1. Cryptolepine hydroiodide, sulfur bioisostere and ring-opened analogs.

Table 1
Training set compounds, experimental activities, and CoMFA predicted activities

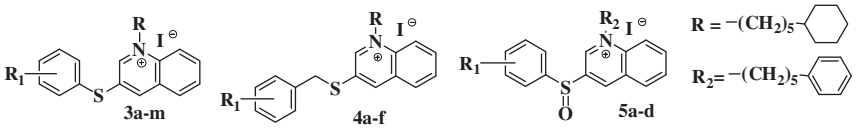

[a]Compound	R_1	Expt IC_{50} (μM) (*Cn*)	Expt.[b] pIC_{50}	Pred.[c] IC_{50} (μM) (*Cn*)	Pred.[c] pIC_{50}	Cytotoxicity (μg/mL [μM])
3a	H	0.966	6.015	0.986	6.006	4.60 [8.89]
3b	*o*-CF_3	3.74	5.427	3.672	5.435	NC
3c	*m*-CF_3	0.683	6.165	0.646	6.190	NC
3d	*p*-CF_3	0.512	6.290	0.579	6.237	NC
3e	*o*-OH	1.88	5.727	1.905	5.720	9.28 [17.4]
3f	*m*-OH	2.34	5.631	2.118	5.674	NC
3g	*p*-OH	1.31	5.882	1.196	5.922	NC
3h	*o*-CH_3	0.565	6.248	0.417	6.379	4.00 [7.53]
3i	*m*-CH_3	0.375	6.425	0.417	6.379	3.70 [6.96]
3j	*p*-CH_3	0.375	6.425	0.417	6.379	2.80 [5.27]
3k	*m*-F	13.2	4.879	16.106	4.793	0.66 [1.23]
3l	*m*-OCH_3	18.5	4.734	19.952	4.700	4.50 [8.22]
3m	*p*-OCH_3	0.731	6.136	0.857	6.067	4.20 [7.67]
4a	H	0.301	6.521	0.307	6.512	NC
4b	*o*-Cl	1.35	5.870	1.588	5.799	NC
4c	*p*-Cl	0.088	7.054	0.139	6.857	1.30 [2.30]
4d	*m*-CH_3	0.769	6.114	0.804	6.095	3.70 [4.95]
4e	*p*-CH_3	0.458	6.339	0.440	6.356	2.70 [6.78]
4f	*p*-CF_3	0.416	6.380	0.428	6.368	4.76 [7.94]
5a	*p*-F	27.5	4.561	32.137	4.493	NC
5b	*m*-CF_3	10.9	4.962	10.046	4.998	NC
5c	*o*-CF_3	9.25	5.034	7.079	5.150	NC
5d	*o*-Br	9.08	5.042	13.520	4.869	NC
5e[*]	*p*-Br	14.9	–	–	–	NC
5f[*]	*p*-CF_3	10.0	–	–	–	10 [21.4]
Cryptolepine[*]		43.3	4.364	–	–	3.20 [8.88]
Amphotericin B[*]		**0.422**	**6.375**	–	–	**6.50 [7.03]**

[a] Compounds **3a**–**m** were previously reported in Refs. 10,11,13.
[b] Experimental pIC_{50}.
[c] Predicted IC_{50} and pIC_{50} from the CoMFA model; NC = not cytotoxic at 10 μg/mL.
[*] These were not included in the training set.

Table 2
Summary of the CoMFA analysis

Statistical parameter	CoMFA model
Cross-validated regression co-efficient, q^2	0.815
# Of components	4
Non cross-validated regression co-efficient, r^2	0.976
Standard error of estimate (SEE)	0.112
Contribution of key parameters	
Steric	0.766
Electrostatic	0.234

against *C. neoformans* were correctly predicted as shown in Table 3 and Figure 4.

A library of 3-(substituted) phenylthio quinolinium iodides (**3**) has shown potential as a new antifungal chemotype demonstrating low cytotoxicity and high potency against a broad spectrum of fungal pathogens and an inherent resistance to the *Candida* genus.[11,12] The original lead compound (**1**), reportedly operates through a unique antifungal mechanism of action which differs from current drugs on the market by intercalating into DNA and inhibiting topoisomerase II.[13] The analogs in this paper are thought to operate through a similar mechanism of action but with a lower degree of intercalation into DNA due to the loss of the flat topography when the B-ring of the tetracyclic structure is opened. This hypothesis may explain the resulting lower cytotoxicity compared to CLP.

The design of **4a** analogs was based on the hypothesis that the distance between the quinolinium and the 3-substituted phenyl moieties in the 3-substituted benzylthio-1-(5-cyclohexylpentyl)quinolin-1-ium iodide (**4a**) scaffold can be exploited to improve potency and decrease toxicity. The introduction of a methylene group was found to produce an optimum chain length since further increase in chain length led to a decrease in anti-cryptococcal activity.[14] In addition, variations in the electronic and hydrophobic

Table 3
Compounds in the test set, their IC_{50} and pIC_{50} values against *C. neoformans* used in the validation of the CoMFA model

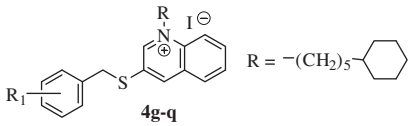

4g-q

[a]Compound	R_1	Exp IC_{50} (μM) (*Cn*)	pIC_{50} Exp	Pred IC_{50} (μM) (*Cn*)	pIC_{50} Pred	Δ(Exp − Pred) IC_{50}	Cytotoxicity IC_{50} (nM)
4g	*p*-OH	9.036	5.044	4.027	5.395	0.351	NC
4h	*p*-*t*-Bu	0.883	6.054	0.887	6.052	0.002	NC
4i	*o*-F	0.948	6.023	1.258	5.900	0.123	NC
4j	*m*-F	0.711	6.148	1.741	5.759	0.389	NC
4k	*p*-F	0.677	6.169	0.622	6.206	0.037	NC
4l	*o*-OCH_3	0.623	6.205	1.757	5.755	0.450	NC
4m	*m*-OCH_3	0.606	6.217	0.568	6.245	0.028	NC
4n	*p*-OCH_3	2.153	5.667	2.173	5.663	0.004	NC
4o	*o*-Br	1.132	5.946	0.997	6.001	0.055	NC
4p	*m*-Br	0.360	6.443	0.273	6.564	0.121	NC
4q	*p*-Br	0.369	6.432	0.267	6.573	0.141	NC

[a] Detailed synthesis of compounds in this table are being published elsewhere. NC = not cytotoxic at 10 μg/mL.

properties of substituents on the A-ring would result in changes in biological activity which can also be exploited to improve drug-like properties. The synthesis and evaluation of the resulting compounds against *C. neoformans* is reported (Table 3) and has provided the basis of the validation of the model.

2. Methods

2.1. Dataset

A training set of 23 compounds was used to generate the CoMFA model. The training set includes compounds from three scaffolds: the phenylthioether (**3**), benzylthioether (**4**), sulfoxide (**5**) ring-opened analogs of cryptolepine and consists of the most potent pharmacophore groups found during the optimization of the lead compound (Fig. 2). The pIC_{50} activity data, originally reported in μg/mL[11,12] and converted to μM for compounds that inhibited *C. neoformans*, had a range of at least 3 log units that provided a starting point in the development of an alignment hypothesis.

2.2. Building aromatic quaternary compounds and structure alignment in Sybyl®

At the beginning of this study, it was discovered that there was no representative atom type for a quaternary aromatic nitrogen atom in the Sybyl software [SYBYL X (1.3)] and thus, it was impossible to build the structure of the salt form of cryptolepine and its derivatives in Sybyl. All attempts to find suitable representations of the quaternary aromatic nitrogen atoms were unsuccessful. Thus, building the structures in the training set was accomplished by extracting cryptolepine (**1**) from the crystal structure of DNA intercalated by cryptolepine (PDB code: 1K9G) to provide the most realistic nitrogen atom representation.[4] The nitrogen atom at position 10 of CLP was replaced with sulfur and ring B was opened. The quaternary aromatic nitrogen atom at position 5 of CLP structure was represented as an sp^2 hybridized nitrogen. Subsequently, the cyclohexylpentyl group was attached to the nitrogen atom and a benzyl group was introduced onto the sulfur atom for compounds in the 3-(substituted) benzylthio quinolinium iodide series (**4a–q**) and the carbon atom types in the quinolinium ring were manually set to aromatic atom types with a +1 charge on the nitrogen. Once built, charges for the compounds were assigned with MMFF94 and minimized by Powell's method and the Tripos force field as implemented in SYBYL X (1.3), terminating with a maximum gradient of 0.05 kcal mol^{-1} Å.[15,16] As expected, this approach resulted in the minimized compounds adopting the correct geometry of the core structure, that is, the quinolinium ring remained flat during the minimization process. After obtaining the common core, the rest of the training set substituted compounds were built from the common core structure.

The minimized compounds were added to a molecular database and aligned using a rigid fit of the common substructure in the training set molecules.[17] Compounds that were out of alignment were adjusted using torsions about the single bond between the sulfur atom and the benzylic carbon. After torsion adjustments were made, the resulting compounds were aligned with the database replacing previous poses (Fig. 3). The quality of the alignment of the training set along with activity diversity are among the most important factors in creating a statistically sound CoMFA model with predictive capabilities.[18,19]

2.3. CoMFA descriptor

The CoMFA steric and electrostatic fields were generated from an active set of compounds that were placed in a 3D grid. At each grid point, the steric and electrostatic energy was calculated for each compound using a probe atom (C.3 with a +1 charge). The cutoff value of 30 kcal/mol eliminated dominant steric and electrostatic energies. The CoMFA method used the partial-least squares (PLS) method to predict activity from the energy values at the grid points and the PLS method correlates the CoMFA fields with the activity values.[10,16] The models with cross-validated q^2 >0.5 are

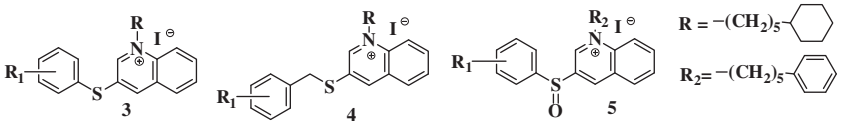

Figure 2. 3-Substituted quinolinium salt scaffolds that make up the compounds used in the CoMFA model.

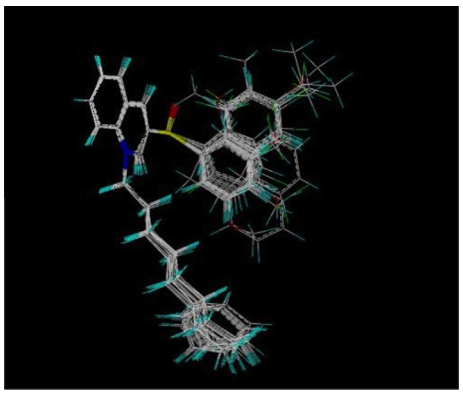

Figure 3. Alignment of structures in the training set.

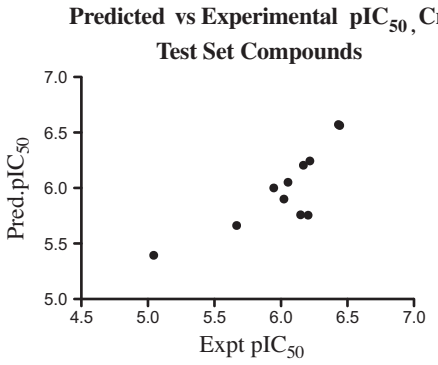

Figure 4. Plot of CoMFA predicted pIC_{50} versus experimental pIC_{50} against *Cn* for the test set.

indicative of a good predictive model. Cross-validation analysis was completed with SAMPLES turned-off and column filtering set to 2.0 kcal mol^{-1} to speed up the analysis. The generation of statistically sound CoMFA models included, at least 3 log units of biological activity, a good alignment, and a common substructure that has the same conformation in all compounds. In addition, torsional angles of the side chains were free to be adjusted to allow for superimposition as much as possible.

The CoMFA descriptor, a 3D descriptor that uses PLS to avoid over-prediction, combines the many variables including steric and electrostatic energies at the grid points from the training set compounds into bins that are represented by a few components.[18,19] It is desirable that, the number of components should be limited to at most four for a data set. The leave-one out (LOO) cross-validation (cv) method pulls out one of the training set compounds, generates a new model, and then predicts the activity of each of the compounds pulled out to ensure that the results of the COMFA model are predictive for compounds that are not in the training set. After several different alignments, the CoMFA model that generated the best statistics was determined by the highest q^2, the lowest standard error of estimate (SEE) and the fewest number of components which was then used to produce the final model. The best model yielded a cv q^2 of 0.815, a SEE of 0.113, and four components (Table 2). The CoMFA calculation for the cv q^2 is found in Eq. 1, where $Y_{predicted}$, Y_{actual}, $Y_{observed}$ and Y_{mean} are the predicted, actual, observed, and mean values of the pIC_{50} activity data. The $\sum(Y_{predicted} - Y_{actual})$ is the predictive sum of squares (PRESS). The COMFA model with the fewest number of components provided the lowest PRESS value.

$$q^2 = 1 - \frac{\sum (Y_{predicted} - Y_{actual})^2}{\sum (Y_{observed} - Y_{mean})^2} \quad (1)$$

2.4. Test set

A test set of 11 compounds was generated from poses of the corresponding training set compounds, minimized and aligned using a rigid fit of the common substructure. The test set compounds were synthesized and their biological activities are shown in Table 3. To determine the validity of the CoMFA model obtained, the experimental activity values were plotted against the predicted activity values (Fig. 4) and the correlation coefficient was calculated using a Prism software.[20]

2.5. Chemistry

The syntheses of compounds **3a**–**m** in the training set were previously reported.[11,12] To obtain the rest of the compounds in the training and test set (**4a**–**f**), 3-iodoquinoline (**6**) was required as the starting material and was obtained by refluxing 3-bromoquinoline in the presence of CuI, NaI and *N*,*N*′-dimethylethylamine in 1,4-dioxane under N_2. A mixture of 3-iodoquinoline, substituted phenyl-methanethiol, CuI and ethylene glycol, in 2-propanol was stirred under microwave irradiation to give substituted 3-(benzylthio)quinolines. Green chemistry was employed as the resulting 3-(substituted benzylthio) quinolines were each alkylated with (5-iodopentyl) cyclohexane in H_2O under microwave irradiation to give substituted 3-(benzylthio)-1-(5-cyclohexylpentyl)quinolin-1-ium iodides (**4a**–**f**). The synthesis of the sulfoxides, **5a**–**d** and the compounds in the test set (**4g**–**q**) are being reported elsewhere (Scheme 1).

3. Results

3.1. CoMFA analysis

The results from the LOO CoMFA analysis are given in Tables 1–3. The cv q^2 was found to be 0.815 with four components, the non-cv r^2 was 0.976, and the SEE was 0.112. The steric contribution was 76.6% of the variance while the electrostatic contribution explains 23.4%. The predicted and experimental biological activities of the training set compounds (pIC_{50}) are also recorded in Table 1.

3.2. Synthesis of compounds 4a–f

The identification of substituted 3-(benzylthio)-1-cyclohexylpentylquinolin-1-ium salts as a target for synthesis derived from the observation that opening the B ring of 5-methylbenzo[4,5]thieno[3,2-*b*]quinolin-5-ium iodide (**2**) and replacing the methyl group with a 5-cyclohexylpentyl group resulted in compounds with increased potency and reduced toxicity compared to the title compound.[11,12] The selection of 5-cyclohexylpentyl moiety as an optimal group was based on our previous work that investigated a homologous series of alkyl groups.[9] Other than the use of new synthetic strategies, that is, microwave synthesis and alkylation in water, the synthesis of the compounds reported here was uneventful.

3.3. Validation of the CoMFA model

3D-QSAR approach has been used as an aid in the design of potent anti-cryptococcal agents based on the structure of the lead compound, 3-phenylthioquinolinium scaffold. Such studies are based on the general principle that semi-superimposable compounds may have similar but different biological activities.[15–18] Several CoMFA models have been generated on a set of compounds with biological activities spread over 3 log units. In the correlation graph Figure 4, the predicted and actual pIC_{50} values are provided,

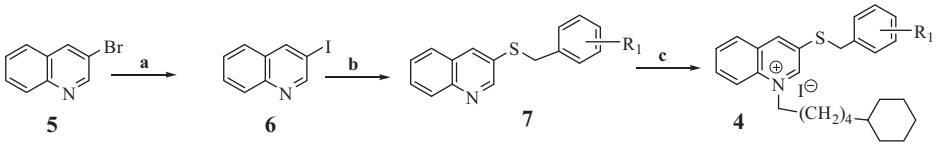

Scheme 1. Synthesis of 3-(substituted benzylthio)quinoline (**7**). Reagents and conditions: (a) CuI, NaI, dioxane, $CH_3NHCH_2CH_2NHCH_3$, reflux under N_2, 110 °C, 48 h; (b) substituted phenylmethanethiol, CuI, Cs_2CO_3, $HOCH_2CH_2OH$, *i*-PrOH, N_2, MWAS, 170 °C, 15 min; (c) $C_6H_{11}(CH_2)_4CH_2$–I, H_2O, MWAS, 170 °C, 15 min.

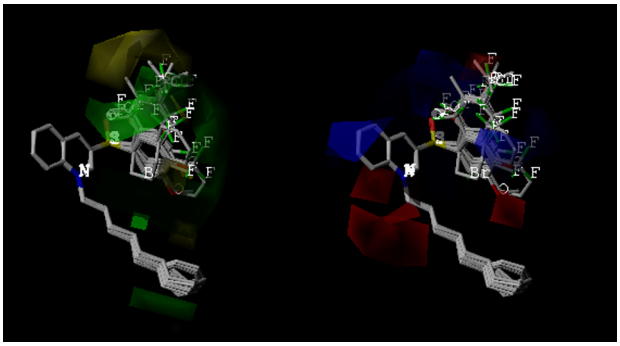

Figure 5. Contour maps with aligned training set compounds.

each point on the graph representing a compound, and points in the upper right area being the most active. Compounds with the highest and lowest pIC_{50} activities were examined in the steric and electrostatic contour maps and the effect of changing functional groups and positions around the phenyl ring A were explored to provide insight into how the various structural entities contribute to activity.

4. Discussion

4.1. CoMFA contour map analysis

CoMFA analysis generates a color-coded contour map that depicts regions in 3D space where changes in the steric and electrostatic fields of a compound correlate strongly with changes in its biological activity (Figs. 5 and 6). The contours of the steric map (Fig. 5) are shown in yellow and green where greater values of biological activity are correlated with more bulk near green and less bulk near yellow. In addition, the electrostatic map (Fig. 5) is shown in red and blue where more positive charge near blue and more negative charge near red are favorable for increased biological activity. In Figure 6, the contours include a large green and small yellow colored contours in the plane of the benzylthio side chain. The *p*-chloro substituent **4c**, is surrounded by a green

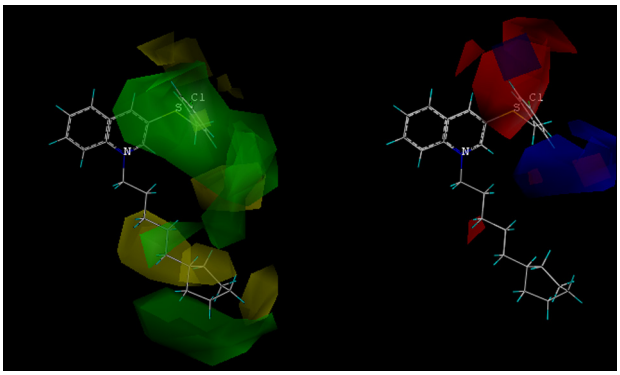

Figure 6. Contour maps with the most active compound.

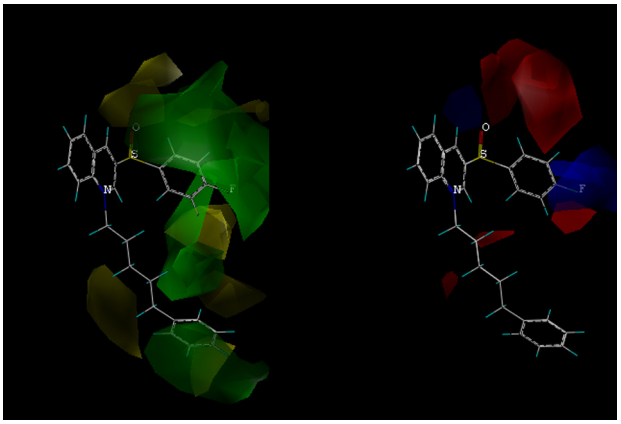

Figure 7. Contour map with least active compound.

contour that favors steric bulk and represents the most potent molecule in the training set.

Also upon inspection of the electrostatic contours, there is a large red area surrounding the electronegative chloro substituent in the *para* position of the phenyl ring. This is consistent with the fact that substitution in the *p*-position enhances activity and electron withdrawing groups ($+\sigma$) increase activity as compared to electron donating groups ($-\sigma$). Thus, together the steric and electrostatic contour maps provide information about the position and type of functional groups that are required for potency and by exploring these 3D spaces with new compounds in silico can lead to new discoveries of more potent inhibitors.

The least active compounds are from the sulfoxide series (**5**). Compound **5a** with a *para* fluoro substituent on the phenyl ring is embedded in the CoMFA contour map shown in Figure 7. The map displays a large green contour slightly out of plane with the small 4-fluoro group on the phenylthio moiety. Inspection of the electrostatic contour map shows that there are large and small red contours and a small blue contour near the phenylthio moiety but little else to explain the observed SAR. There are no clear indications in this pose as to why the sulfoxides are inactive and any suggestions here would be considered as pure speculation.

4.2. Structure–activity relationship

The results of the biological evaluation of the compounds suggest that 3-(benzylthio)-1-(5-cyclohexylpentyl)quinolin-1-ium group constitutes the pharmacophore for the **4a**–**q** series since the 1-(5-cyclohexylpentyl)quinolin-1-ium moiety by itself does not produce activity.[9] In this manuscript, the electronic and hydrophobic space around the phenyl ring of the benzylthio moiety was explored and indicates that functional groups with positive sigma and increasing pi values increase potency and especially when placed at the *p*-position. Oxidation of the sulfur directly attached to the quinolinium ring (**3a**–**m**) to a sulfoxide (**5a**–**f**), such as might occur during metabolism in vivo, attenuates activity.

It is unclear whether the attenuation of activity observed with the sulfoxide has any relation to the electronic effect on the

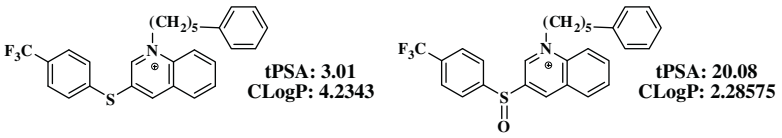

Figure 8. Estimate of the physicochemical characteristics of a thioether versus a sulfoxide.

quinolinium scaffold. However, estimates of *C*log *P* and tPSA for a typical sulfide and its corresponding sulfoxide (Fig. 8), suggest significant decrease in *C*log *P* (4.2–2.3) and an increase in tPSA (3.01–20.1). Given that both parameters correlate well with passive molecular transport through membranes and, hence allow the prediction of transport properties of drugs across bio-membranes,[21] it is tempting to suggest that the decrease in activity from the thioether to sulfoxide may be related to the ability of the latter to cross biological membranes.

This study has led to the confirmation of substituted 1-(5-cyclohexylpentyl)-3-{[(substituted)benzyl]-thio}quinolin-1-ium iodide as a viable scaffold for the design and synthesis of novel anticryptococcal agents. An approach to obtaining an atom type for quaternary aromatic nitrogen has been demonstrated and used in building appropriate structures for this CoMFA study. A predictive CoMFA model was obtained with a cross-validated q^2 of 0.81 and r^2 of 0.98. The model was subsequently validated by predicting 11 designed analogs which were synthesized, screened and the resulting anticryptococcal activities were shown to have a significant correlation with that predicted by the model (R = 0.82). Substitution on the benzyl group and especially at the *para* position with increasing pi and positive σ values enhance potency and combined with their low cytotoxicity, hints at 3-(benzylthio)-1-(5-cyclohexylpentyl)quinolin-1-ium scaffold constituting a new chemotype which can further be exploited to obtain analogs with higher potency, low cytotoxicity and overall better therapeutic anti-cryptococcal profile.

5. Experimental section

5.1. Chemistry

The melting points were determined in °C on an Electrothermal MEL-TEMP 3.0 device without correction. ^{1}H NMR spectra of intermediates and final products in $CDCl_3$, DMSO-d_6, or CD_3OD were recorded on a Varian 300 MHz Mercury NMR Spectrometer. Chemical shifts relative to TMS and the internal standard are given in δ (ppm) and *J*-values are recorded in Hertz. Elemental analyses were carried out by Atlantic Microlab, Inc., Norcross, GA, and were within ±0.4% of the theory unless otherwise noted. All reagents and solvents were purchased from Sigma–Aldrich, Fisher Scientific or Alfa Aesar and were used without further purification. Reactions were monitored by analytical thin layer chromatography (TLC) carried out on Sigma–Aldrich TLC plates coated with F_{254} silica gel. Purified intermediates and final products showed one spot.

5.1.1. Procedure for the synthesis of 3-iodoquinoline, 6

The key intermediate, 3-iodoquinoline was obtained from the commercially 3-bromoquinoline using a literature method previously utilized in our lab.[7] ^{1}H NMR ($CDCl_3$): δ 9.03 (d, 1H, J = 2.4 Hz), 8.54–8.53 (m, 1H), 8.08–8.04 (m, 1H), 7.76–7.69 (m, 2H), 7.59–7.53 (m, 1H).

5.1.2. General procedure for the synthesis of 3-[(substituted) benzylthio]quinoline, 7a–f

Substituted phenylmethanethiol (2.59 mmol) was added to a stirred solution of 3-iodoquinoline (0.794 g, 3.11 Hzmmol), CuI (0.049 g, 0.259 mmol), Cs_2CO_3 (1.69 g, 5.17 mmol), ethylene glycol (0.321 g, 5.17 mmol) in 2-propanol (5 mL) and heated using microwave irradiation at 170 °C for 15 min under N_2. After cooling, aqueous NH_4Cl (10 mL) was added to quench the reaction, followed by extraction with EtOAc and water then washed with brine (10 mL), and dried over anhydrous Na_2SO_4. The solvent from the combined organic fractions was removed in vacuo and the residue was purified by Flash chromatography (12 g silica column) using a 10% EtOAc:Hexane mobile phase, which provided the pure 3-(substituted benzylthio) quinoline as oils.

5.1.2.1. 3-(Benzylthio)quinoline, 7a. Yield 77.1%; ^{1}H NMR ($CDCl_3$): δ 8.78 (s, 1H), 8.04 (d, 1H, J = 8.7 Hz), 7.98 (s, 1H), 7.70–7.66 (m, 3H), 7.52 (t, 1H, J = 6.0 Hz), 7.29–7.26 (m, 4H), 4.19 (s, 2H).

5.1.2.2. 3-((2-Chlorobenzyl)thio)quinoline, 7b. Yield 70.0%; ^{1}H NMR ($CDCl_3$): δ 8.78 (s, 1H), 8.06 (d, 1H, J = 9.0 Hz), 7.98 (s, 1H), 7.72–7.69 (m, 2H), 7.53 (t, 1H, J = 8.4 Hz), 7.26–7.17 (m, 4H), 4.14 (s, 2H).

5.1.2.3. 3-((4-Chlorobenzyl)thio)quinoline, 7c. Yield 50.5%; ^{1}H NMR ($CDCl_3$): δ 8.78 (s, 1H), 8.05 (d, 1H, J = 8.7 Hz), 7.98 (s, 1H), 7.72–7.70 (m, 1H), 7.69–7.66 (m, 1H), 7.45 (t, 1H, J = 9.0 Hz), 7.26–7.25 (m, 2H), 7.23–7.18 (m, 2H), 4.14 (s, 2H).

5.1.2.4. 3-((3-Methylbenzyl)thio)quinoline, 7d. Yield 73.5%; ^{1}H NMR ($CDCl_3$): δ 8.79 (s, 1H), 8.06 (d, 1H, J = 8.7 Hz), 7.95 (s, 1H), 7.66–7.61 (m, 2H), 7.52–7.46 (m, 1H), 7.18–7.13 (m, 1H), 7.04–7.08 (m, 3H,), 4.13 (s, 2H), 2.15 (s, 3H).

5.1.2.5. 3-((4-Methylbenzyl)thio)quinoline, 7e. Yield 71.6%; ^{1}H NMR ($CDCl_3$): δ 8.78 (s, 1H), 8.05 (d, 1H, J = 8.4 Hz), 7.99 (s, 1H), 7.68–7.63 (m, 2H), 7.54–7.49 (m, 1H), 7.17 (s, 2H,), 7.08 (d, 2H, J = 7.8 Hz), 4.16 (s, 2H), 2.30 (s, 3H).

5.1.2.6. 3-((4-(Trifluoromethyl)benzyl)thio)quinoline, 7f. Yield 55.7%; ^{1}H NMR ($CDCl_3$): δ 8.79 (s, 1H), 8.06 (d, 1H, J = 8.4 Hz), 7.98 (s, 1H), 7.73–7.67 (m, 2H), 7.57–7.52 (m, 1H), 7.37 (d, 2H, J = 8.1 Hz), 7.04–6.98 (m, 2H), 4.21 (s, 2H).

5.1.3. General procedure for the synthesis of 3-[(substituted) benzylthio]-1-(5-cyclohexyl-pentyl) quinolin-1-ium iodide, 4a–f

5-Iodopentyl cyclohexane (0.16 g, 0.572 mmol) was added to a well-stirred solution of 3-(substituted benzylthio)quinoline, **7a–f** (0.381 mmol) in H_2O (5 mL) and subjected to microwave irradiation at 170 °C for 15 min. After cooling to room temperature, EtOAc (10 mL) was added to the microwave reaction vial and the top organic fraction was collected. The organic layer was then sonicated until a yellow salt crystallized out of solution, the resulting crude product was then vacuum filtered using the solvents EtOAc, followed by Et_2O giving the product 3-(substituted benzylthio)-1-(5-cyclohexypentyl)quinolin-1-ium iodide, **4a–f**.

5.1.3.1. 3-(Benzylthio)-1-(5-cyclohexylpentyl)quinolin-1-ium iodide, 4a. Yield 58%, mp 108–110 °C; ^{1}H NMR (DMSO-d_6): δ 9.59 (s, 1H), 9.22 (s, 1H), 8.52 (d, 1H, J = 9.0 Hz), 8.31 (d, 1H,

J = 5.1 Hz), 8.18–8.12 (m, 1H), 8.01–7.96 (m, 1H), 7.41 (d, 2H, J = 7.35 Hz), 7.34–7.21 (m, 3H), 4.96 (t, 2H, J = 7.5 Hz), 4.55 (s, 2H), 2.01–1.81 (m, 2H), 1.71–1.53 (m, 5H), 1.51–1.25 (m, 4H), 1.21–1.01 (m, 6H), 0.92–0.70 (m, 2H). Anal. Calcd for $C_{27}H_{34}INS$: C, 61.01; H, 6.45; N, 2.64. Found: C, 60.94; H, 6.62; N, 2.61.

5.1.3.2. 3-((2-Chlorobenzyl)thio)-1-(5-cyclohexylpentyl)quinolin-1-ium iodide, 4b. Yield 17.2%; mp 110–112 °C; ^{1}H NMR (DMSO-d_6) δ 9.64 (s, 1H), 9.27 (s, 1H), 8.54 (d, 1H, J = 8.92 Hz), 8.32 (dd, 1H, J = 1.45, 8.28 Hz), 8.19 (ddd, 1H, J = 1.51, 6.99, 8.80 Hz), 8.04–7.97 (m, 1H), 7.47 (ddd, 2H, J = 1.74, 6.16, 7.54 Hz), 7.36–7.20 (m, 2H), 4.98 (t, 2H, J = 8.78 Hz), 4.59 (s, 2H), 1.95–1.82 (m, 2H), 1.70–1.53 (m, 6H), 1.43–1.19 (m, 3H), 1.13 (m, 6H), 0.90–0.69 (m, 2H). Anal. Calcd for $C_{27}H_{33}INSCl$: C, 57.30; H, 5.88; N, 2.47. Found: C, 57.17; H, 5.77; N, 2.49.

5.1.3.3. 3-((4-Chlorobenzyl)thio)-1-(5-cyclohexylpentyl)quinolin-1-ium iodide, 4c. Yield 59.0%, mp 102–104 °C; ^{1}H NMR (DMSO-d_6): δ 9.57 (s, 1H), 9.24 (s, 1H), 8.52 (d, 1H, J = 9.0 Hz), 8.35–8.29 (dd, 1H, J = 1.2, 8.4 Hz), 8.19–8.14 (m, 1H), 8.02–7.97 (m, 1H), 7.44–7.40 (m, 2H), 7.41–7.35 (m, 2H), 4.98 (t, 2H, J = 9.0 Hz), 4.54 (s, 1H), 1.99–1.79 (m, 2H), 1.69–1.48 (m, 6H), 1.45–1.21 (m, 4H), 1.20–1.00 (m, 6H), 0.90–0.70 (m, 2H). Anal. Calcd for $C_{27}H_{33}ClINS$: C, 57.30; H, 5.88; N, 2.47. Found: C, 57.35; H, 5.81; N, 2.58.

5.1.3.4. 1-(5-Cyclohexylpentyl)-3-((3-methylbenzyl)thio)quinolin-1-ium iodide, 4d. Yield 5.4%; mp 100.4–102.3 °C; ^{1}H NMR (DMSO-d_6): δ 9.60 (s, 1H), 9.23 (s, 1H), 8.52 (d, 1H, J = 9.3 Hz), 8.31 (d, 1H, J = 7.2 Hz), 8.19–8.14 (m, 1H), 7.99 (t, 1H, J = 7.5 Hz), 7.23–7.15 (m, 3H), 7.06–7.04 (m, 1H), 4.99 (t, 2H, J = 7.5 Hz), 4.52 (s, 2H), 2.23 (s, 3H), 1.93–1.93 (m, 2H), 1.69–1.66 (m, 5H), 1.31–1.28 (m, 4H), 1.14–1.15 (m, 6H), 0.87–0.76 (m, 2H). Anal. Calcd for $C_{28}H_{36}INS$: C, 61.64; H, 6.65; N, 2.57. Found: C, 61.76; H, 6.81; N, 2.63.

5.1.3.5. 1-(5-Cyclohexylpentyl)-3-((4-methylbenzyl)thio)quinolin-1-ium iodide, 4e. Yield 56.0%, mp 100–102 °C; ^{1}H NMR (DMSO-d_6): δ 9.57 (s, 1H), 9.21 (s, 1H), 8.51 (d, 1H, J = 9.0 Hz), 8.30 (d, 1H, J = 8.4 Hz), 8.18–8.12 (m, 1H), 8.01–7.96 (m, 1H), 7.31–7.26 (m, 2H), 7.12–7.08 (m, 2H), 4.98 (t, 2H, J = 8.7 Hz), 4.50 (s, 2H), 2.22 (s, 3H), 2.01–1.83 (m, 2H), 1.75–1.55 (m, 6H), 1.48–1.22 (m, 4H), 1.20–1.05 (m, 5H), 0.91–0.70 (m, 2H). Anal. Calcd for $C_{28}H_{36}INS$: C, 61.64; H, 6.65; N, 2.57. Found: C, 61.72; H, 6.76; N, 2.66.

5.1.3.6. 1-(5-Cyclohexylpentyl)-3-((4-(trifluoromethyl)benzyl)thio)quinolin-1-ium iodide, 4f. Yield 18.9%, mp 126–128 °C; ^{1}H NMR (DMSO-d_6): δ 9.59 (s, 1H), 9.26 (s, 1H), 8.53 (d, 1H, J = 8.4 Hz), 8.30 (d, 1H, J = 8.4 Hz), 8.17 (t, 1H, J = 7.5 Hz), 8.03–7.97 (m, 1H), 7.66 (d, 2H, J = 8.7 Hz), 7.63 (d, 2H, J = 8.7 Hz), 4.96 (t, 2H, J = 7.2 Hz), 4.64 (s, 2H), 1.96–1.80 (m, 2H), 1.70–1.50 (m, 5H), 1.4–1.25 (m, 4H), 1.2–1.0 (m, 6H), 0.90–0.70 (m, 2H). Anal. Calcd for $C_{28}H_{33}F_3INS$: C, 56.09; H, 5.55; N, 2.34. Found: C, 56.34; H, 5.56; N, 2.40.

6. Biological activity

6.1. Antifungal testing

C. neoformans ATCC 90113 was obtained from the American Type Culture Collection (Manassas, VA). Susceptibility testing was performed using a modified version of the CLSI methods as described by Samoylenko et al.[22] Briefly, DMSO solutions of samples were serially diluted in saline and transferred in duplicate to 96-well microplates. Microbial suspensions were diluted in Sabouraud Dextrose broth to afford desired colony forming units/mL. After adding microbial cultures to the samples affording a final volume of 200 μL and final test concentration starting with 20 μg/mL, plates were read at 530 nm prior to and after incubation using the Biotek Powerwave XS plate reader (Bio-Tek Instruments, Vermont). Growth (saline only), solvent, and blank (media only) controls were included on each test plate. The drug control amphotericin B (ICN Biomedicals, Ohio) was included in each assay. IC_{50}s (concentrations that afford 50% inhibition relative to controls) were calculated using XLfit 4.2 software (IDBS, Alameda, CA) using fit model 201.

6.2. Cytotoxicity assay

In vitro cytotoxicity was determined against mammalian kidney fibroblast (VERO) cells. The assay was performed in 96-well tissue culture-treated microplates and compounds were tested up to a highest concentration of 10 mg/mL as described earlier.[23] In brief, cells (25,000 cells/well) were seeded to the wells of the plate and incubated for 24 h. Samples were added and plates were again incubated for 48 h. The number of viable cells was determined by the Neutral Red dye assay. IC_{50} values were determined from dose curves of growth inhibition versus concentration. Doxorubicin was used as a positive control, while DMSO was used as the negative (vehicle) control.

Acknowledgments

We acknowledge research support from the National Institutes of Health, National Institute of Allergy and Infectious Diseases, Research Centers at Minority Institutions (RCMI) Grant number G12 RR 03020, and Title III Grant to Florida A&M University. This research was also supported in part by the Pharmaceutical Research Center NIH/NCRR 1C06-RR12512-01 Grant. One of us, S.B. is grateful for financial support from the AFPE. We thank Dr. Wang Zhang, NMR facility manager responsible for instrumentation for the generation of NMR spectra of compounds in this paper, Mrs Barbara Bricker, for proof reading the manuscript and Ms. Marsha Wright for antifungal testing. Antifungal testing was supported by the NIH, NIAID, Division of AIDS, Grant No. AI 27094.

References and notes

1. Kaplan, J. E.; Benson, C.; Holmes, K. H.; Brooks, J. T.; Pau, A.; Masur, H. *MMWR Recomm. Rep.* **2009**, *58*, 1.
2. Sarmiento, G. P.; Vitale, R. G.; Afeltra, J.; Moltrasio, G. Y.; Moglioni, A. G. *Eur. J. Med. Chem.* **2011**, *46*, 101.
3. Barrett, A. G. M.; Doubleday, W. W.; Hamprecht, D.; Kasdorf, K.; Tustin, G. J.; White, A. J. P.; Williams, D. J. *Chem. Commun. (Camb)* **1997**, 1693.
4. Kathiravan, M. K.; Salake, A. B.; Chothe, A. S.; Dudhe, P. B.; Watode, R. P.; Mukta, M. S.; Gadhwe, S. *Bioorg. Med. Chem.* **2012**, *20*, 5678.
5. (a) Kumar, E. V.; Etukala, J. R.; Ablordeppey, S. Y. *Mini-Rev. Med. Chem.* **2008**, *8*, 538; (b) Ablordeppey, S. Y.; Hufford, C. D.; Borne, R. F.; Dwuma-Badu, D. *Planta Med.* **1990**, *56*, 416; (c) Mardenborough, L. G.; Fan, P. C.; Ablordeppey, S. Y.; Nimrod, A.; Clark, A. M. *Med. Chem. Res.* **1999**, *9*, 118; (d) Ablordeppey, S. Y.; Fan, P.; Li, S.; Clark, A. M.; Hufford, C. D. *Bioorg. Med. Chem.* **2002**, *10*, 1337.
6. Lisgarten, J. N.; Coll, M.; Portugal, J.; Wright, C. W.; Aymami, J. *Nat. Struct. Biol.* **2002**, *9*, 57.
7. Zhu, X. Y.; Mardenborough, L. G.; Li, S.; Khan, A.; Zhang, W.; Fan, P.; Jacob, M.; Khan, S.; Walker, L.; Ablordeppey, S. Y. *Bioorg. Med. Chem.* **2007**, *15*, 686.
8. Mazu, T. K.; Etukala, J. R.; Zhu, X. Y.; Jacob, M. R.; Khan, S. I.; Walker, L. A.; Ablordeppey, S. Y. *Bioorg. Med. Chem.* **2011**, *19*, 524.
9. (a) Ablordeppey, S. Y.; Fan, P.; Clark, A. M.; Nimrod, A. *Bioorg. Med. Chem.* **1999**, *7*, 343; (b) Mardenborough, L. G.; Zhu, X. Y.; Fan, P.; Jacob, M. R.; Khan, S. I.; Walker, L. A.; Ablordeppey, S. Y. *Bioorg. Med. Chem.* **2005**, *13*, 3955.
10. Mazu, T. K.; Etukala, J. R.; Jacob, M. R.; Khan, S. I.; Walker, L. A.; Ablordeppey, S. Y. *Eur. J. Med. Chem.* **2011**, *46*, 2378.
11. Boateng, C. A.; Eyunni, S. V.; Zhu, X. Y.; Etukala, J. R.; Bricker, B. A.; Ashfaq, M. K.; Jacob, M. R.; Khan, S. I.; Walker, L. A.; Ablordeppey, S. Y. *Bioorg. Med. Chem.* **2011**, *19*, 458.

12. Boateng, C. A.; Zhu, X. Y.; Jacob, M. R.; Khan, S. I.; Walker, L. A.; Ablordeppey, S. Y. *Eur. J. Med. Chem.* **2011**, *46*, 1789.
13. Dassonneville, L.; Bonjean, K.; De Pauw-Gillet, M. C.; Colson, P.; Houssier, C.; Quetin-Leclercq, J.; Angenot, L.; Bailly, C. *Biochemistry* **1999**, *38*, 7719.
14. Bolden, S.; Zhu, X. Y.; Etukala, J. R.; Boateng, C.; Mazu, T.; Flores-Rozas, H.; Jacob, M. R.; Khan, S. I.; Ablordeppey, S. Y. *Eur. J. Med. Chem.* **2013**. under review.
15. (a) Cramer, R. D.; Patterson, D. E.; Bunce, J. D. *J. Am. Chem. Soc.* **1988**, *110*, 5959; (b) SYBYL-X 1.2, T. I., 1699 South Hanley Rd., St. Louis, Missouri, 63144, USA.
16. Murugesan, V.; Prabhakar, Y. S.; Katti, S. B. *J. Mol. Graph. Model.* **2009**, *27*, 735.
17. Carrieri, A.; Muraglia, M.; Corbo, F.; Pacifico, C. *Eur. J. Med. Chem.* **2009**, *44*, 1477.
18. Lu, P.; Wei, X.; Zhang, R. *Eur. J. Med. Chem.* **2010**, *45*, 3413.
19. Clark, M.; Cramer, R. D.; Vanopdenbosch, N. *J. Comput. Chem.* **1989**, *10*, 982.
20. GraphPad. Correlation Analysis, was Performed Using GraphPad Prism Version 5 for Mac OSX, Graphpad Software, San Diego California USA, http://www.graphpad.com.
21. Ertl, P.; Rohde, B.; Selzer, P. *J. Med. Chem.* **2000**, *43*, 3714.
22. Samoylenko, V.; Jacob, M. R.; Khan, S. I.; Zhao, J.; Tekwani, B. L.; Midiwo, J. O.; Walker, L. A.; Muhammad, I. *Nat. Prod. Commun.* **2009**, *4*, 791.
23. Mustafa, J.; Khan, S. I.; Ma, G.; Walker, L. A.; Khan, I. A. *Lipids* **2005**, *40*, 375.